CHINESE OPTICS LETTERS

Vol. 19, No. 11 | November 2021

Adjustable-free and movable Nd:YVO_4 thin disk laser based on the telecentric cat's eye cavity

Wei Wang (王 巍)[1,2,†], Yongxi Gao (高勇喜)[1,2,†], Di Sun (孙 迪)[1,2], Xiao Du (杜 潇)[1,2], Jie Guo (郭 洁)[1], and Xiaoyan Liang (梁晓燕)[1,3,*]

[1] State Key Laboratory of High Field Laser Physics, Shanghai Institute of Optics and Fine Mechanics, Chinese Academy of Sciences, Shanghai 201800, China

[2] Center of Materials Science and Optoelectronics Engineering, University of Chinese Academy of Sciences, Beijing 100049, China

[3] School of Physical Science and Technology, ShanghaiTech University, Shanghai 200031, China

*Corresponding author: liangxy@siom.ac.cn

Received April 6, 2021 | Accepted April 24, 2021 | Posted Online August 24, 2021

In this paper, we propose and demonstrate an adjustable-free and movable Nd:YVO_4 thin disk laser based on the telecentric cat's eye cavity. We design a V-shaped laser cavity containing two reflectors with Nd:YVO_4 thin disks as the gain medium. The experimental results from the traditional plane-plane cavity, plane-telecentric cat's eye cavity, and double telecentric cat's eye cavity are compared. They show that plane-telecentric cat's eye cavity laser can keep operating at the adjustable-free range of −6° to +6°, which is up to 60 times better than that of traditional plane-plane cavity. In the double telecentric cat's eye case, the adjustable-free range is improved to −13° to +13°. Additionally, in the case of the double telecentric cat's eye cavity, the output telecentric cat's eye can achieve free movement within the horizontal range of ±20 mm.

Keywords: thin disk laser; telecentric cat's eye; adjustable-free laser.

DOI: 10.3788/COL202119.111403

1. Introduction

The laser diode pumped all-solid-state laser has the advantages of compact structure, high reliability, high beam quality, and high conversion efficiency, which can be used for laser ranging, lidar, laser communication, and high-energy laser weapons. The resonator is an important part of the laser oscillator. The role of the resonator is to provide positive feedback of the axial laser mode and to ensure the single mode (or a few axial modes) oscillations of the laser. In general, it is very difficult to make a laser work ideally because it is quite difficult to adjust the two end mirrors of the resonator to a completely parallel state. Besides, when the cavity mirror of the resonator is slightly disturbed, the output of the laser will fluctuate greatly, even disappear. For all conventional plane-plane, plane-concave, and concave-concave cavity lasers, these problems are inevitable. The alignment and power stability issues for the all-solid-state laser limit its applications in many fields. These problems are especially serious in low-gain lasers.

In addition to alignment and power stability issues, the movable resonator has special application values. The researchers proposed a resonant beam charging (RBC) technology that can safely transmit multi-watt wireless power over multi-meter distance, also known as distributed laser charging (DLC)[1,2]. The RBC is a wireless power transfer technology that transfers power through the intra-cavity resonant beam. The mobility of the resonant cavity is the premise of the RBC system to realize movable wireless power transmission. For the RBC system, the transmission power and efficiency when the output mirror moves along the axis of the resonant cavity have been demonstrated[3]. However, the mobility of the RBC system along the horizontal direction needs further study.

Adjustable-free solid lasers have been reported several times. In some Nd:$Y_3Al_5O_{12}$ (Nd:YAG) lasers, Porro prisms or cube-corner prisms have been used as the reflector of the laser resonator[4,5]. Cube-corner prisms can improve the stability of the system and achieve the adjustable-free function, but there are two disadvantages. Firstly, the vertex of the cube-corner prism is not an effective reflection point and cannot reflect the incident beam. Therefore, there is a dark hole in the center of the output beam profile of the lasers formed by the cube-corner prism. Second, the tiny processing error on three mutually perpendicular surfaces may cause a considerable amount of loss. In addition to Porro prisms and cuber-corner prisms, the cat's eye reflector can also be used for an adjustable-free laser. The optical advantages of the cat's eye reflector have been demonstrated[6,7]. The cat's eye reflector is usually used as an outside mirror in the interferometer systems to reflect the beam, in which the cat's eye reflector does not form a laser cavity as a resonator mirror[8]. Recently, there have been many attempts to use

the cat's eye reflector as the resonator mirror. In 1965, Li and Smith proposed the cat's eye cavity laser[9]. However, the article only wants to select the transverse mode of the laser output by two diaphragms and does not mention the stability problem of the resonator. In 1994, Dimakov *et al.* proposed a cat's eye cavity CO_2 laser. However, the high-power density on the back of the cat's eye reflector may damage the coating, and the conic optical elements require very high manufacturing accuracy, which hinders its application[10–12]. In 1998, Fermigier *et al.* proposed a cat's eye cavity external-cavity semiconductor laser[13]. However, the system structure composed of a cylindrical lens and a grating is too complex. In 2005, Xu *et al.* proposed an adjustable-free cat's eye cavity He–Ne laser and studied its stability[14]. The cat's eye cavity can overcome the shortcomings of the cube-corner prism, but the adjustable-free range is limited, and mobile alignment cannot be achieved.

In this paper, we propose and demonstrate an adjustable-free and movable Nd:YVO_4 thin disk laser based on the telecentric cat's eye cavity. A series of comparative experiments are conducted based on the traditional plane-plane cavity, plane-telecentric cat's eye cavity, and double telecentric cat's eye cavity. The traditional alignment problem has been well solved, and the adjustable-free range is greatly improved. Besides, the resonator based on the double telecentric cat's eye can achieve horizontal mobile alignment and even multi-end simultaneous output.

2. Telecentric Cat's Eye Reflector

The cat's eye reflector is composed of a convex lens and a concave mirror. The focal length of the convex lens, the radius of curvature of the concave mirror, and the distance between the two elements are all equal. Figure 1(a) shows the reflection of the cat's eye reflector to the obliquely incident beam. As shown in Fig. 1(b), the telecentric cat's eye reflector is composed of a convex lens and a plane mirror. The distance between the convex lens and the plane mirror is equal to the focal length of the convex lens. Obviously, the normal incident paraxial beam will be reflected by the telecentric cat's eye reflector along the

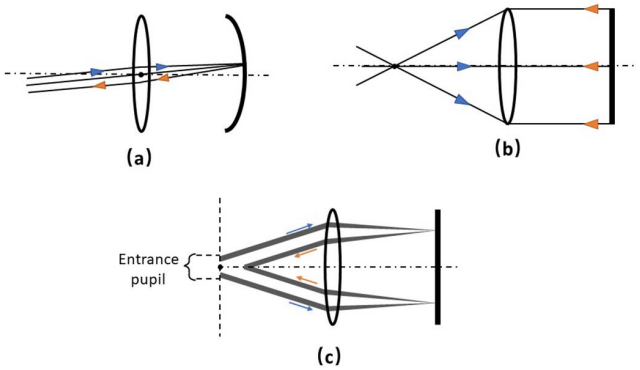

Fig. 1. (a) Cat's eye reflector, (b) a telecentric cat's eye reflector, and (c) obliquely incident beam to a telecentric cat's eye reflector.

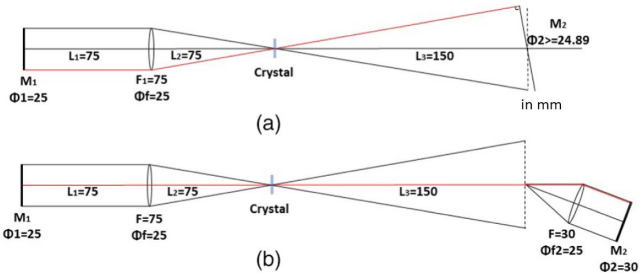

Fig. 2. (a) Plane-telecentric cat's eye cavity laser and (b) double telecentric cat's eye cavity laser.

entrance way. As shown in Fig. 1(c), even for an oblique incident light beam, the telecentric cat's eye reflector can provide high parallelism for the incident and the reflected beam, which is impossible for a traditional laser resonator mirror. Therefore, when the telecentric cat's eye reflector is used as a resonator mirror, if there is tiny disturbance that sways the mirror for a small angle, this advantage can help reduce the negative influence. In other words, the telecentric cat's eye reflector can achieve the adjustable-free function. Besides, the double telecentric cat's eye cavity is also expected to achieve mobile alignment.

We build a laser model, as shown in the Fig. 2(a). At one end of the cavity, a telecentric cat's eye with a focal length of 75 mm is used. The output mirror M_2 has a rotation function, and the rotation angle depends on the aperture and focal length of the telecentric cat's eye reflector. When the focal length of the telecentric cat's eye structure is 75 mm, and the size is 25 mm, the maximum rotation angle of M_2 is $\arctan(12.5/75) = 9°27'44''$. When the diameter of M_2 is φ_2, the rotation is

$$\theta = \arcsin\left(\frac{\varphi_2}{2L_3}\right).$$

With the length of L_3 increasing, the rotation angle of M_2 decreases. The M_2 in Fig. 2(a) is replaced by an output telecentric cat's eye structure. The double telecentric cat's eye laser is shown in Fig. 2(b). The output telecentric cat's eye contains an $F_2 = 30$ mm lens. The rotation angle of the double telecentric cat's eye structure laser depends on the output telecentric cat's eye structure. When the component size of the telecentric cat's eye structure is 25 mm, the maximum rotation angle of the output telecentric cat's eye is $\arcsin(12.5/30) = 22°37'12''$. At the same time, the output telecentric cat's eye can support translation motion, and, when $L_3 = 150$ mm, the translation motion distance of the output telecentric cat's eye is 25 mm.

3. Experimental Results and Discussion

A traditional V-shaped symmetrical plane-plane cavity with the cavity length of 150 mm was used for the experiment. The gain medium was a self-made double-pass pumped Nd:YVO_4 thin disk. A $15\,\text{mm} \times 15\,\text{mm} \times (4+1)$ mm single diffusion-bounded $YVO_4 - $ Nd:YVO_4 with 0.5% (atomic fraction) doping

concentration *a*-cut Nd:YVO_4 crystal was used, and the *c* axis of the crystal was perpendicular to the working plane. The thickness of YVO_4 was 4 mm, and the thickness of Nd:YVO_4 was 1 mm. The undoped end face of the crystal was anti-reflection coated at both the laser and pump wavelengths. At the same time, the doped end face of the crystal was high-reflection coated at 1064 nm and 880 nm. The design of the heat sink and pump system was as described in Ref. [15]. The pump light was imaged to a 1.1 mm diameter spot at the undoped end face of the crystal. The unabsorbed pump power was collected into a dump.

The output power at the initial position was 17.15 W when the pump current was 40 A. We rotated the output mirror. The positive sign means that the output mirror rotates counterclockwise, and the negative sign means that the output mirror rotates clockwise. As shown in Fig. 3, the output power did not change much when the rotation angle of the output mirror was within ±0.04°. However, once the rotation angle exceeded ±0.04°, the output power rapidly decreased. Eventually, when the rotation angle exceeded ±0.1°, the laser output disappeared. The traditional laser resonant cavity is very sensitive to slight perturbation, and the angle rotation of more than ±0.1° will make the resonant cavity invalid. The inset in Fig. 3 is the output beam profile at the initial position.

For comparison, we tested the plane-telecentric cat's eye cavity. Theoretically, the adjustable-free range depends on the output coupling mirror geometry and the distance between the output coupling mirror and the gain medium. The theory concludes that the adjustable-free range is 12°. The experimental arrangement is shown in Fig. 4. The plane-telecentric cat's eye cavity was formed by a telecentric cat's eye reflector and an output mirror. The telecentric cat's eye reflector was formed by a lens with $F = 75$ mm and a plane mirror, and both diameters were 25 mm. The length between the lens and the plane mirror was 75 mm. The gain medium was placed at the focal point of the lens. The telecentric cat's eye reflector was equivalent to a 4F system. Therefore, the telecentric cat's eye reflector was equivalent to a high-reflection coated mirror closely attached to the gain

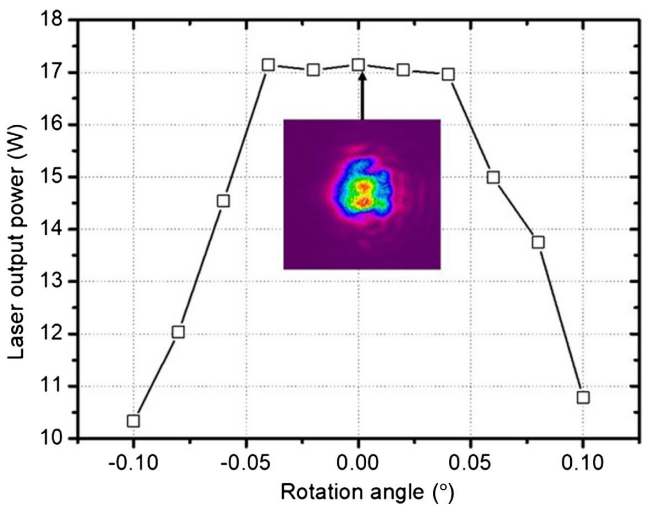

Fig. 3. Laser output power versus rotation angle in plane-plane cavity.

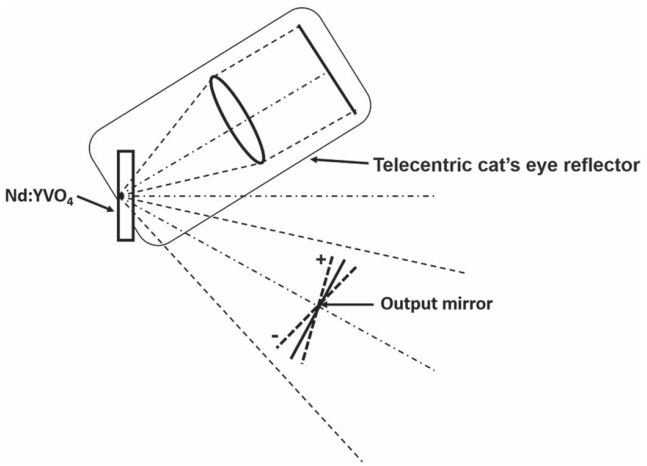

Fig. 4. Schematic of plane-telecentric cat's eye cavity.

medium. The diameter of the output mirror was 30 mm, and the output coupling efficiency was 30%. The distance between the output mirror and the gain medium was 150 mm.

When the pump current was 18 A, the output power at the initial position was 4.97 W. Figure 5 was the output power versus the rotation angle in the plane-telecentric cat's eye cavity. When the output mirror rotated in the counterclockwise direction, the laser output power decreased slowly as the rotation angle increased. When the rotation angle exceeded 6.6°, the laser output power decreased rapidly until it disappeared after further increasing the rotation angle. When the output mirror rotated in the clockwise direction, consistent with the counterclockwise direction, the laser output power decreased as the rotation angle increased. The difference was that the laser output power decreases faster when rotating clockwise than counterclockwise.

Theoretically, when rotating counterclockwise, the angle between the optical path and the axis of the gain medium decreases, and the angle with respect to the axis of the cat's

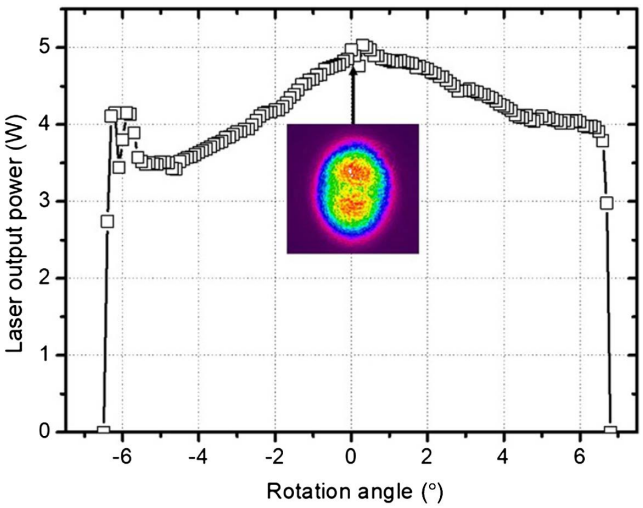

Fig. 5. Laser output power versus rotation angle in plane-telecentric cat's eye cavity.

eye reflector increases. The reduction in aberration caused by the gain medium can partially offset the increase in aberration in the cat's eye reflector, so the laser power decreased more slowly. In contrast, when rotating clockwise, the angle between the optical path and the axis of the gain medium and the angle between the optical path and the cat's eye reflector both increased. At the same time, the aberrations of the gain medium and the cat's eye reflector will increase, so the laser power dropped faster. In addition, when the rotation angle exceeded −5.4°, the laser output power increased as the rotation angle increased until it reached a maximum value of 4.15 W. At this time, we observed that two polarization states of the laser output simultaneously. When the rotation angle exceeded −6.4°, the laser output power quickly decreased until it disappeared. The adjustable-free ranges of positive and negative angles were approximately symmetrical. The adjustable-free range of the plane-telecentric cat's eye cavity was more than 60 times higher than that of the traditional plane-plane cavity. The inset in Fig. 5 was the output beam profile at the initial position. When the power dropped in two directions, the output beam profile did not change much, and there was no black hole in the output beam profile.

As for high power, when the pumping current reached 28 A, the output power at the initial position was 9.74 W. As shown in Fig. 6, with the output power increased, the adjustable-free range was unchanged. In addition, the changing trend of laser output power with the rotation angle was the same as that of low power. The inset in Fig. 6 was the output beam profile at the initial position. The experimental results of the adjustable-free range were consistent with the theoretical calculations.

In the double telecentric cat's eye cavity laser, we replaced the output mirror in the plane-telecentric cat's eye cavity laser with the output telecentric cat's eye. The difference was that the plane mirror in the output telecentric cat's eyes was the output mirror in the plane-telecentric cat's eye cavity laser. In the output telecentric cat's eye, the focal length of the lens was 30 mm, and the diameter was 25 mm. The lens and output mirror were installed

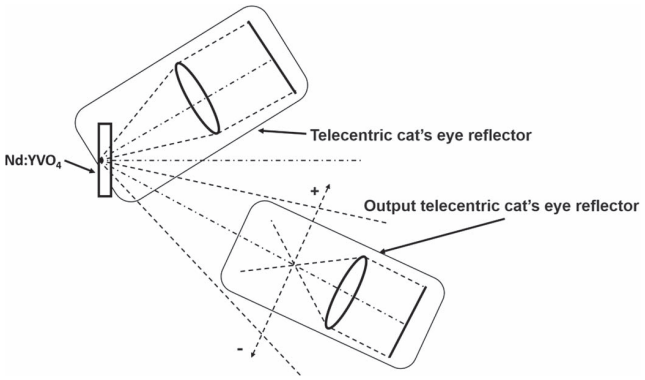

Fig. 7. Schematic of double telecentric cat's eye cavity.

together through a sleeve. The distance between the focal point of the second telecentric cat's eye and the gain medium was 150 mm. The schematic diagram of the double telecentric cat's eye cavity laser is shown in Fig. 7.

As for the plane-telecentric cat's eye cavity laser, the adjustable-free range of the output telecentric cat's eye structure was measured (the line passing the lens focal point and perpendicular to the lens normal plane serves as the axis of rotation). The output power at the initial position was 10.19 W when the pump current was 28 A. As shown in Fig. 8, in the range of ±6°, the rotation of the output telecentric cat's eye reflector had little effect on the laser output power and the output beam quality. When the rotation angle exceeded ±6°, as the rotation angle increased, the output power decreased slowly, and output beam quality degraded until it disappeared. The changes in laser output power and beam quality when rotating clockwise and counterclockwise displayed symmetry. The adjustable-free range reached ±13°. Compared with traditional plane-plane cavity, the adjustable-free range was increased by approximately 130 times. In addition, compared with the plane-telecentric cat's eye cavity, the adjustable-free range was

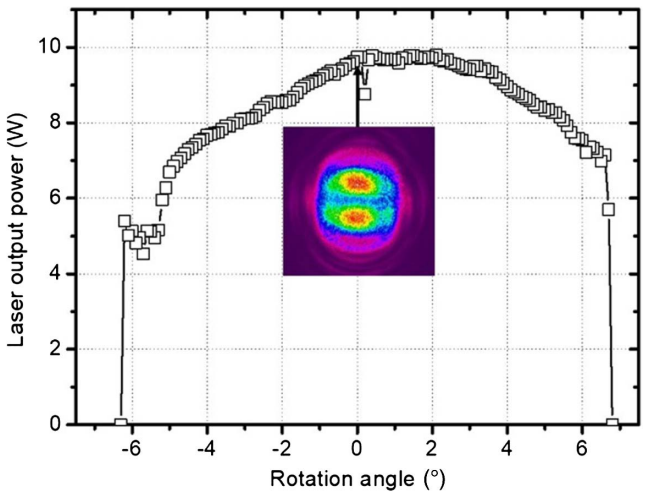

Fig. 6. Laser output power versus rotation angle in plane-telecentric cat's eye cavity (high power).

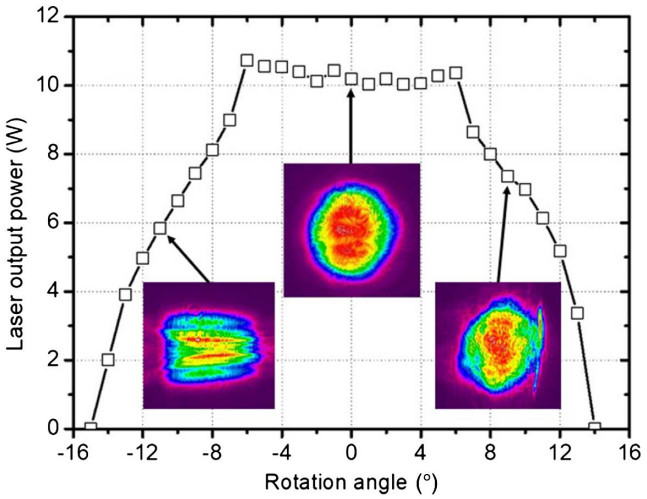

Fig. 8. Laser output power versus rotation angle in double telecentric cat's eye cavity.

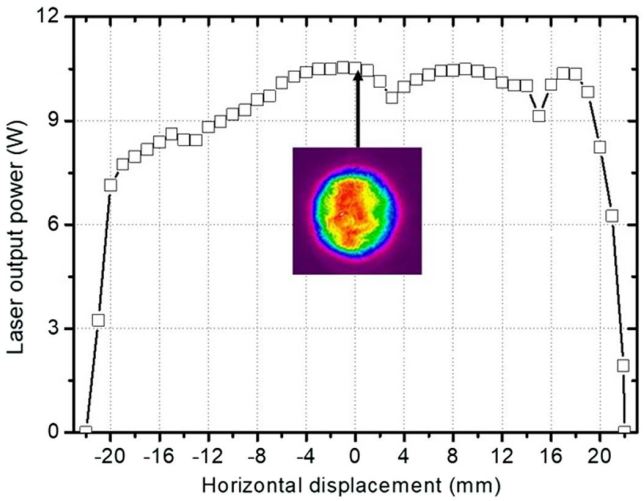

Fig. 9. Laser output power versus horizontal displacement.

also increased about twice. Besides, the output power of the laser stayed relatively stable within an angular variation range of ±6°. Therefore, the double telecentric cat's eye cavity not only improved the adjustable-free range, but also greatly improved the stability of the output power. The inset in Fig. 8 is the output beam profile at the initial position. Theoretically, the adjustable-free range of the double telecentric cat's eye cavity was 22.5°. The experimental adjustable-free range was smaller than the theoretical prediction due to aberrations.

The double telecentric cat's eye cavity not only effectively increased the adjustment-free range and improved the power stability, but also achieved the movability of the output telecentric cat's eye. The theory calculated that the movability of the adjustable-free range was ±25 mm. As shown in Fig. 9, the output power changed when the output telecentric cat's eye moved in the horizontal direction perpendicular to the axis. The output power at the initial position was 10.51 W. The movable range of the output telecentric cat's eye was about ±20 mm. The negative sign means moving away from the normal of the gain medium, and the positive sign means moving towards the normal of the gain medium. When moving in the positive direction, the laser output power fluctuated around 10 W until the horizontal displacement exceeded 19 mm, and the laser output power dropped rapidly until it disappeared. When moving in the negative direction, the laser output power decreased slowly as the moving distance increased, and the output power dropped rapidly until it disappeared after the moving distance exceeded 19 mm. Theoretically, when moving in the positive direction, the angle between the optical path and the axis of the gain medium decreased, and the angle between the optical path and the axis of the telecentric cat's eye increased. In this case, the reduction in the aberration caused by the gain medium can partially offset the increase in the aberration in the cat's eye reflector, thereby keeping the output power relatively stable. When moving in the negative direction, the angle between the optical path and the axis of the gain medium and the angle between the optical path and the axis of the cat's eye reflector were increased, and the aberrations caused by the gain medium and the cat's eye reflector increased. Thus, the laser output power decreased as the moving distance increased. In summary, compared with the traditional plane-plane cavity and the plane-telecentric cat's eye cavity, the double telecentric cat's eye cavity can achieve the adjustment-free and mobile alignment of the output telecentric cat's eye within the coverage angle of 15°. In addition, it is also expected to achieve multi-end simultaneous output within the coverage.

4. Conclusion

In this article, we demonstrated an adjustable-free and movable Nd:YVO_4 thin disk laser based on the telecentric cat's eye cavity. Our goal is studying the mobility of the RBC system. Generally, when the resonant cavity is not optimized, the output beams are multi-mode. All of the output beams in these several lasers are not optimized, so it is possible to obtain single mode output beams after optimization. The experimental results from the traditional plane-plane cavity, plane-telecentric cat's eye cavity, and double telecentric cat's eye cavity were compared. They show that the plane-telecentric cat's eye cavity laser can keep operating at the adjustable-free range of −6° to 6°, which was up to 60 times better than that of the traditional plane-plane cavity. In the double telecentric cat's eye case, the adjustable-free range was improved to −13° to +13°. Additionally, in the case of the double telecentric cat's eye cavity, the output telecentric cat's eye can achieve free movement within the horizontal range of ±20 mm. In summary, the advantages of the Nd:YVO_4 thin disk laser based on the telecentric cat's eye cavity is adjustable-free and movable. Besides, it is also expected to achieve multi-end simultaneous output. These advantages are very important to achieve mobile wireless power transmission based on all-solid-state lasers.

Acknowledgement

This work was supported by the National Natural Science Foundation of China (NSFC) (Nos. 61775223 and 11974367), Strategic Priority Research Program of Chinese Academy of Sciences (No. XDB1603), and Shanghai Science and Technology Innovation Action Plan Project (No. 19142202500).

†These authors contributed equally to this work.

References

1. Q. Liu, J. Wu, P. Xia, S. Zhao, W. Chen, Y. Yang, and L. Hanzo, "Charging unplugged: will distributed laser charging for mobile wireless power transfer work?" IEEE Veh. Technol. Mag. **11**, 36 (2016).
2. Q. Zhang, W. Fang, Q. Liu, J. Wu, P. Xia, and L. Yang, "Distributed laser charging: a wireless power transfer approach," IEEE Internet Things J. **5**, 3853 (2018).
3. W. Wang, Q. Zhang, H. Lin, M. Liu, X. Liang, and Q. Liu, "Wireless energy transmission channel modeling in resonant beam charging for IOT devices," IEEE Internet Things J. **6**, 3976 (2019).
4. L. Ramos-Izquierdo, J. L. Bufton, and P. Hayes, "Optical system design and integration of the Mars Observer Laser Altimeter," Appl. Opt. **33**, 307 (1994).

5. Y. Cheng, B. Chen, and X.-B. Wang, "Study on diode pumped solid laser (DPSL) with alignment-free resonator," Chin. J. Lasers **30**, 973 (2003).
6. R. Beer and D. Marjaniemi, "Wavefronts and construction tolerances for a cat's-eye retroreflector," Appl. Opt. **5**, 1191 (1966).
7. J. J. Snyder, "Paraxial ray analysis of a cat's-eye retroreflector," Appl. Opt. **14**, 1825 (1975).
8. M. L. Biermann, W. S. Rabinovich, R. Mahon, and G. C. Gilbreath, "Design and analysis of a diffraction-limited cat's-eye retroreflector," Opt. Eng. **41**, 1655 (2002).
9. T. Li and P. W. Smith, "Mode selection and mode volume enhancement in a gas laser with internal lens," Proc. IEEE **53**, 399 (1965).
10. S. A. Dimakov, S. I. Kliment'ev, V. I. Kuprenyuk, I. B. Orlova, V. V. Sergeev, and V. E. Sherstobitov, "Resonator with low sensitivity to misalignments," Proc. SPIE **2257**, 187 (1994).
11. V. E. Sherstobitov, A. A. Ageichik, V. D. Bulaev, S. A. Dimakov, M. N. Gerke, D. A. Goryachkin, V. P. Kalinin, I. Koval, E. N. Paryshev, Y. A. Rezunkov, N. A. Romanov, A. Y. Rodionov, V. V. Stepanov, and V. V. Zemlyanykh, "Phase conjugation in a high-power E-beam-sustained CO_2 laser," Proc. SPIE **1841**, 135 (1992).
12. S. A. Dimakov, S. I. Klimentev, and I. V. Khloponina, "Cavity with a cat's-eye reflector based on elements of conical optics," J. Opt. Technol. **69**, 536 (2002).
13. B. Fermigier, G. Lucas-Leclin, J. Dupont, F. Plumelle, and M. Houssin, "Self-aligned external-cavity semiconductor lasers for high resolution spectroscopy," Opt. Commun. **153**, 73 (1998).
14. Z. Xu, S. Zhang, Y. Li, and W. Du, "Adjustment-free cat's eye cavity He–Ne laser and its outstanding stability," Opt. Express **13**, 5565 (2005).
15. W. Wang, D. Sun, X. Du, J. Guo, and X. Liang, "High-power operation of double-pass pumped Nd:YVO_4 thin disk laser," High Power Laser Sci. Eng. **8**, e10 (2020).